

CHAPTER 3

APPLICATIONS AND SIMULATIONS

3.1 Introduction

It has been seen that a graphical method for the determination of the frequency response of a certain class of nonlinear systems has been developed for handling particular types of nonlinear terms. The use of this method will be applied to the nonlinear system described in Fig. 2.1 for different kinds of nonlinear transfer functions such as dead-zone, relay with dead-zone, relay with hysteresis and dead-zone, backlash, and saturation. These nonlinear configurations have been given in Appendix A. Typical examples of the determination of frequency responses of nonlinear systems are described in the following sections.

3.2 Dead Zone

It is known that dead zone describes a range of input for which the response is zero Fig. 3.2 describes this situation, which is also known as threshold, or flat spot. This type of nonlinearity is generally found in any dc motor with armature control.

3.2.1 Example

Consider a typical nonlinear system as shown in Fig. 3.1

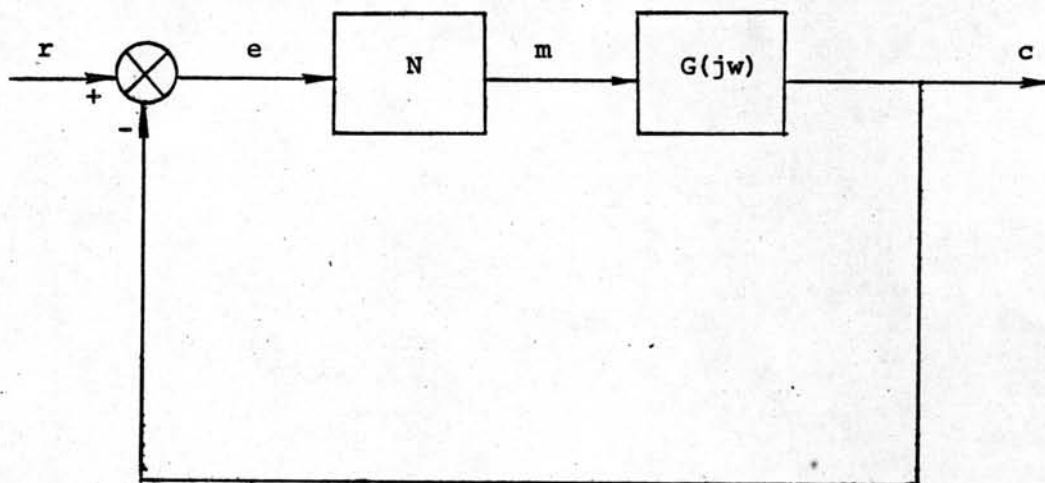


Fig. 3.1 A typical nonlinear system with dead zone.

The input signal, in this case, is

$$r = 3.75 \sin \omega t \quad (3.1)$$

The parameters of the characteristic shown in Fig. 3.2 are

$$\left. \begin{aligned} b &= 1.5 \\ n &= 3 \end{aligned} \right\} \quad (3.2)$$

The linear transfer function is

$$G(j\omega) = \frac{1}{(j\omega)^2} \quad (3.3)$$

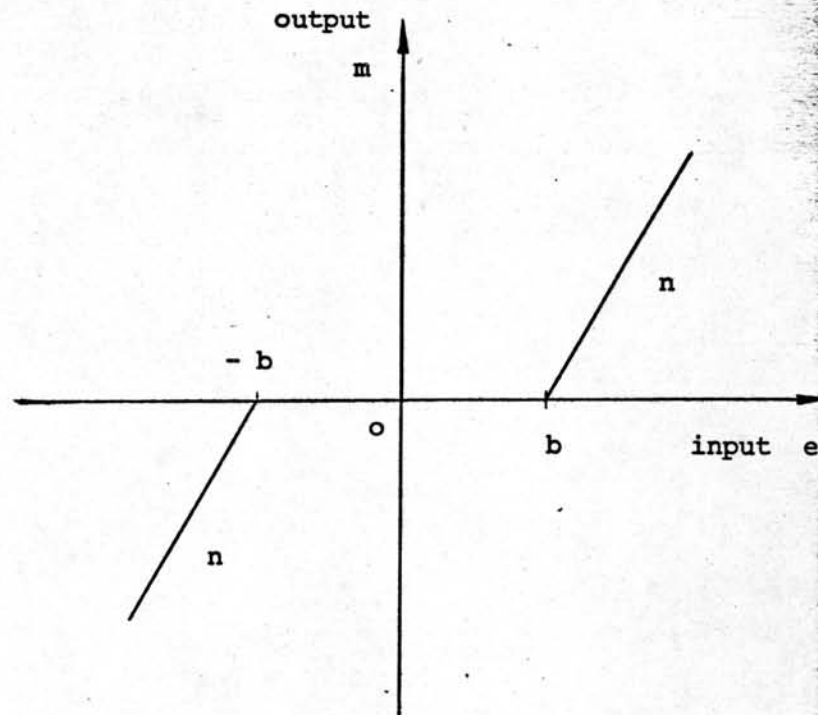


Fig. 3.2 A dead-zone characteristic.

The family of circle curves and the linear transfer function are plotted in the same complex plane graph in Fig.3.3. The output frequency response of this nonlinear system for various values of frequency w has been calculated by eqn. (2.13) and also listed in Table 3.1. The output response is also plotted in Fig. 3.4. It can be seen from Fig. 3.4 that there is no jump phenomena appearance in this nonlinear system.

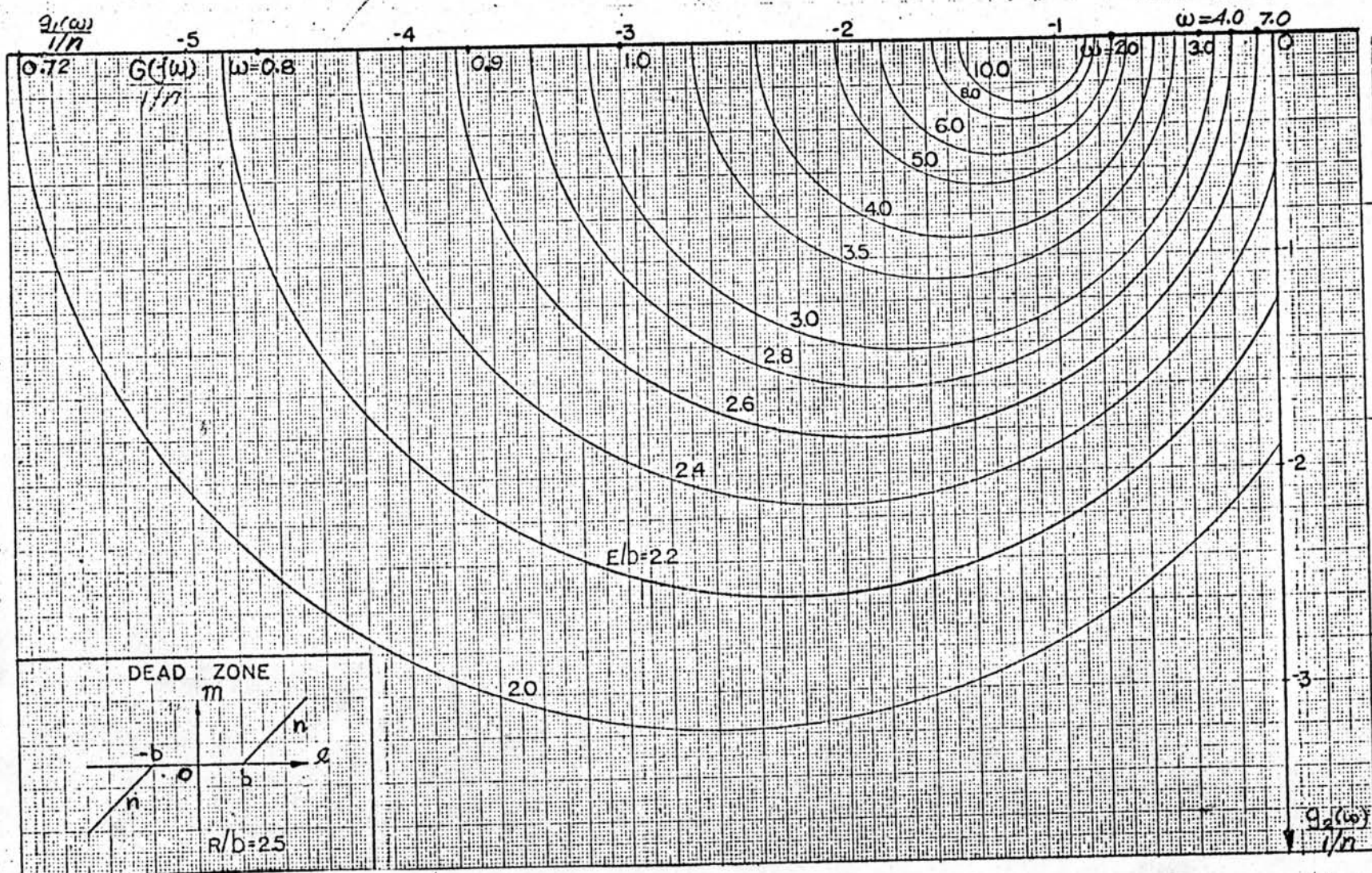


Fig. 3.3 Family of circle curves for dead zone and the curve of $G(j\omega) = \frac{1}{(j\omega)^2}$

Table 3.1 Calculated result of example in section 3.2.1.

E/b	w	$\frac{G(jw)}{1/n}$	$G(jw) Keq(E)$	$1+G(jw) Keq(E)$	$ \frac{C}{R} $	$ \frac{C}{R} $ db	θ
2.0	0.72	-5.76	-2.25	-1.25	1.80	5.11	0°
2.2	0.79	-4.84	-2.14	-1.14	1.88	5.48	0°
2.4	0.89	-4.21	-2.04	-1.04	1.96	5.85	0°
3.5	1.06	-2.67	-1.71	-0.71	2.14	7.64	0°
5.0	1.22	-2.01	-1.50	-0.50	3.00	9.54	0°
10.0	1.44	-1.44	-1.26	-0.26	4.85	13.71	0°
6.0	2.00	-1.74	-1.37	-0.37	3.70	11.36	0°
3.5	2.56	-0.45	-0.29	+0.71	0.41	-7.74	180°
3.0	3.30	-0.27	-0.16	+0.84	0.19	-14.42	180°
2.8	4.00	-0.19	-0.11	+0.89	0.12	-18.4	180°
2.6	7.00	-0.07	-0.04	+0.96	0.04	-27.60	180°

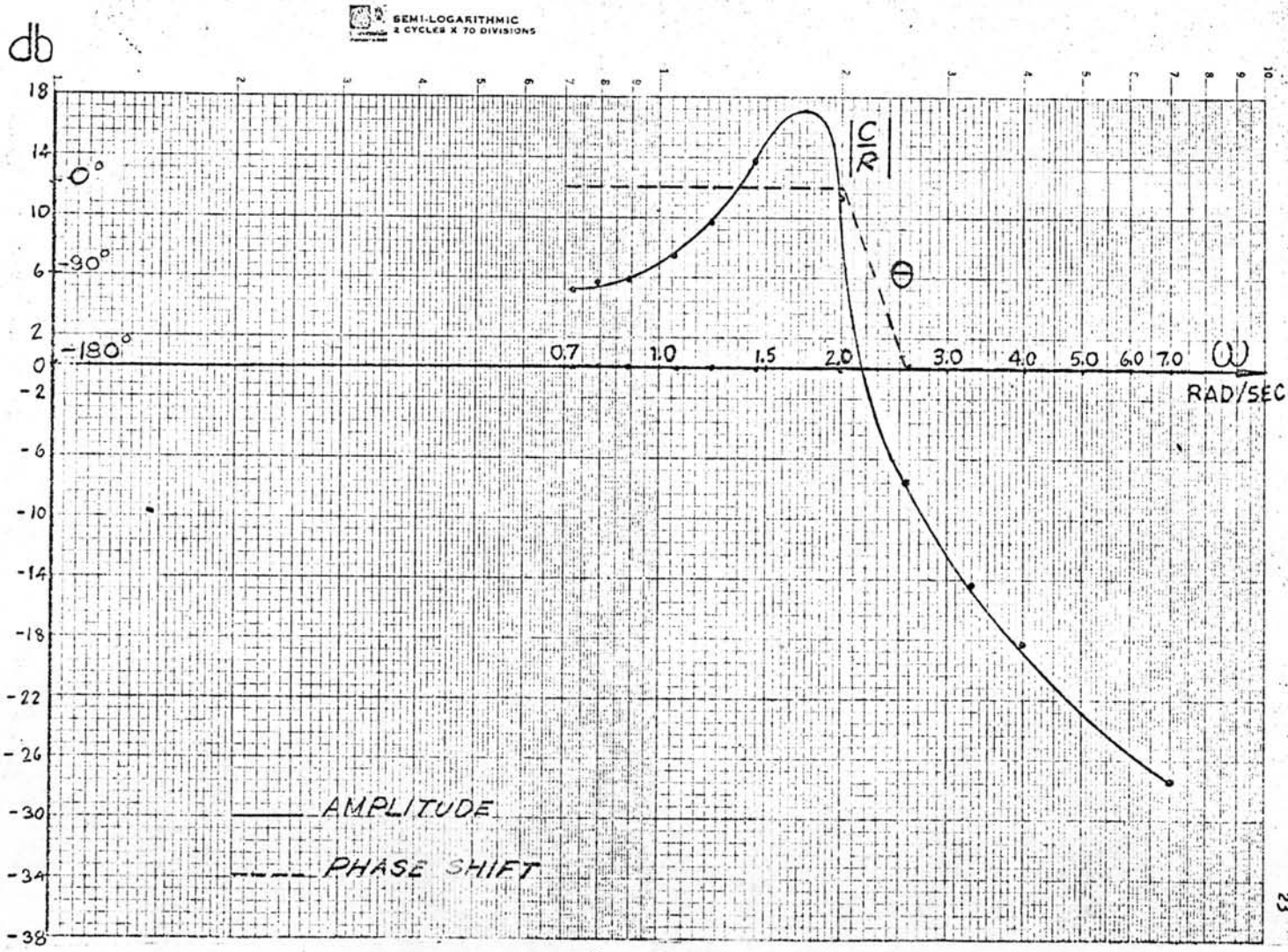


Fig. 3.4 Output frequency response of nonlinear system described in Fig.3.1 and 3.2

3.3 Ideal Relay

The ideal relay characteristic without dead zone or hysteresis has appearance as shown in Fig. 3.5.

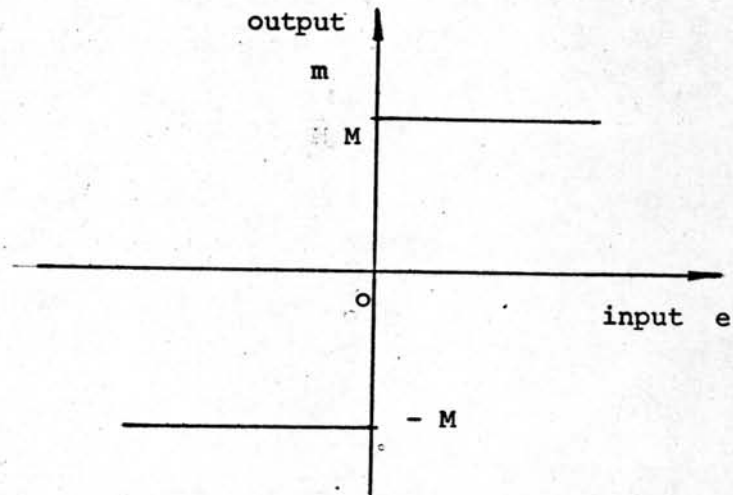


Fig. 3.5 An ideal relay characteristic.

3.3.1 Example

Consider a typical nonlinear system as shown in Fig. 3.6.

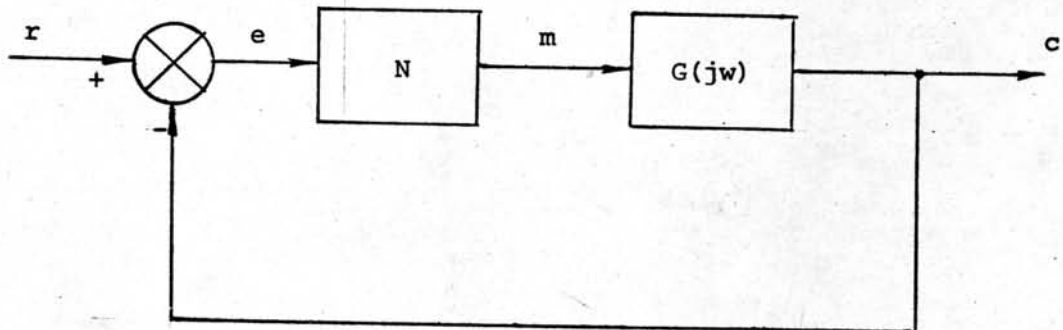


Fig. 3.6 A typical nonlinear system with ideal relay.

The input signal is

$$r = 1.5 \sin \omega t \quad (3.4)$$

The parameters of the characteristic shown in Fig. 3.5 are

$$M = 1.0 \quad (3.5)$$

The linear transfer function is

$$G(j\omega) = \frac{100}{j\omega(10 + j\omega)} \quad (3.6)$$

In this example the family of circle curves and the new linear transfer function, $\frac{G(j\omega)}{1/M}$, are plotted in the same complex graph in Fig. 3.7. The output frequency response of this nonlinear system for various values of frequency ω has been calculated by eqn. (2.13) and also listed in Table 3.2, the output response is also plotted in Fig. 3.8. It can be seen that there is no jump response phenomena occurs in this system.

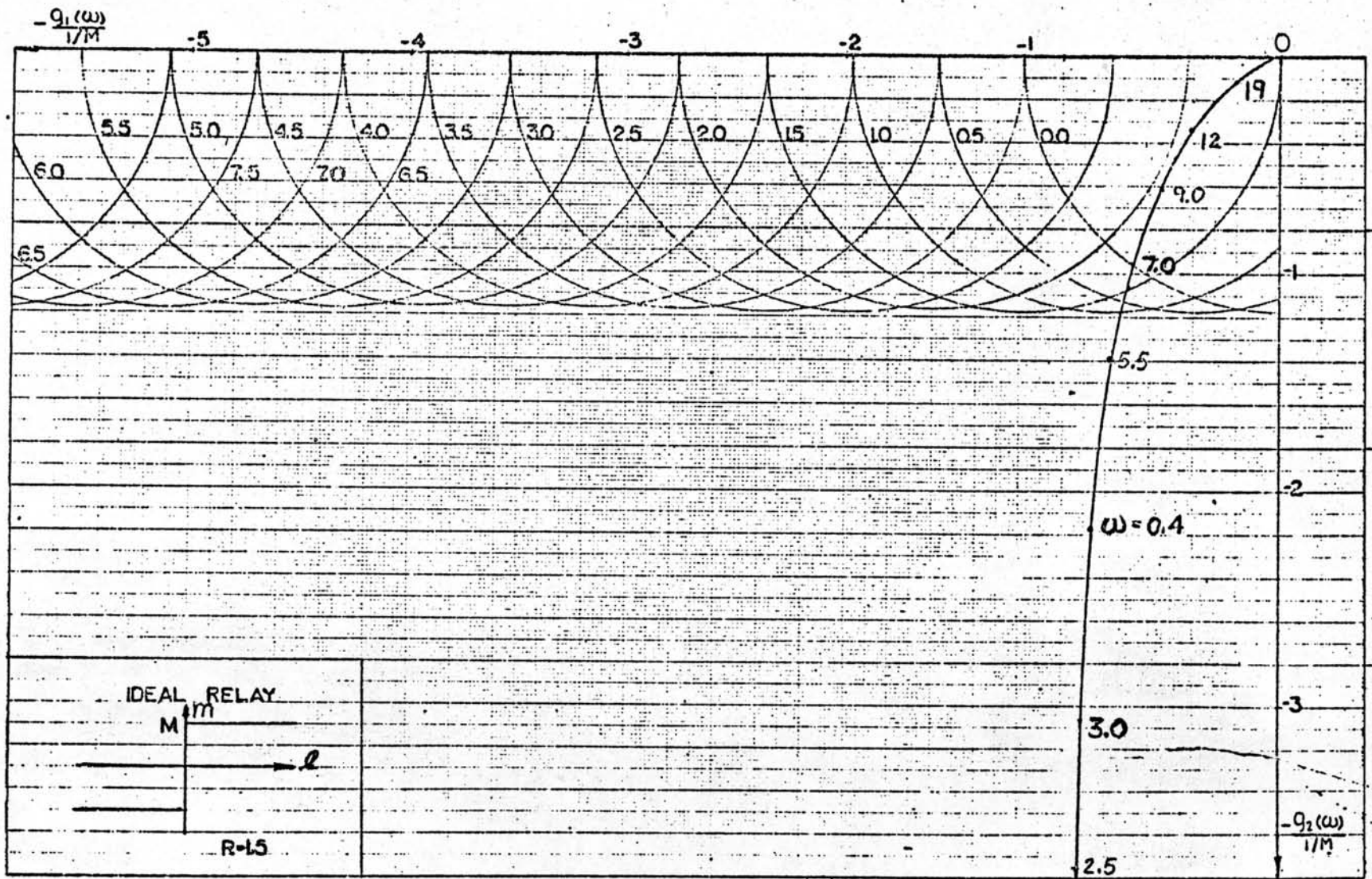


Fig. 3.7 Family of circle curves for ideal relay and the curve of
 $G(j\omega) = \frac{100}{j\omega(10+j\omega)}$

Table 3.2 Calculated results of example in section 3.3.1

E	w	$G(j\omega)K_{eq}(E)$	$1+G(j\omega)K_{eq}(E)$	$ C/R $	$ C/R $ db	θ
1.0	6.1	1.77 \angle 239.9	1.5 \angle -87.7	1.18	1.44	-32.4°
0.5	6.2	3.41 \angle 237.6	3.0 \angle -73.9	1.14	1.11	-48.5°
1.5	6.5	1.09 \angle 236.6	1.0 \angle -66.3	1.09	0.75	-57.1°
1.57	12	0.43 \angle 221.2	0.74 \angle -22.4	0.58	-4.73	-116.4°
1.75	19	0.17 \angle 207.6	0.85 \angle -5.4	0.20	-13.98	-147.0°

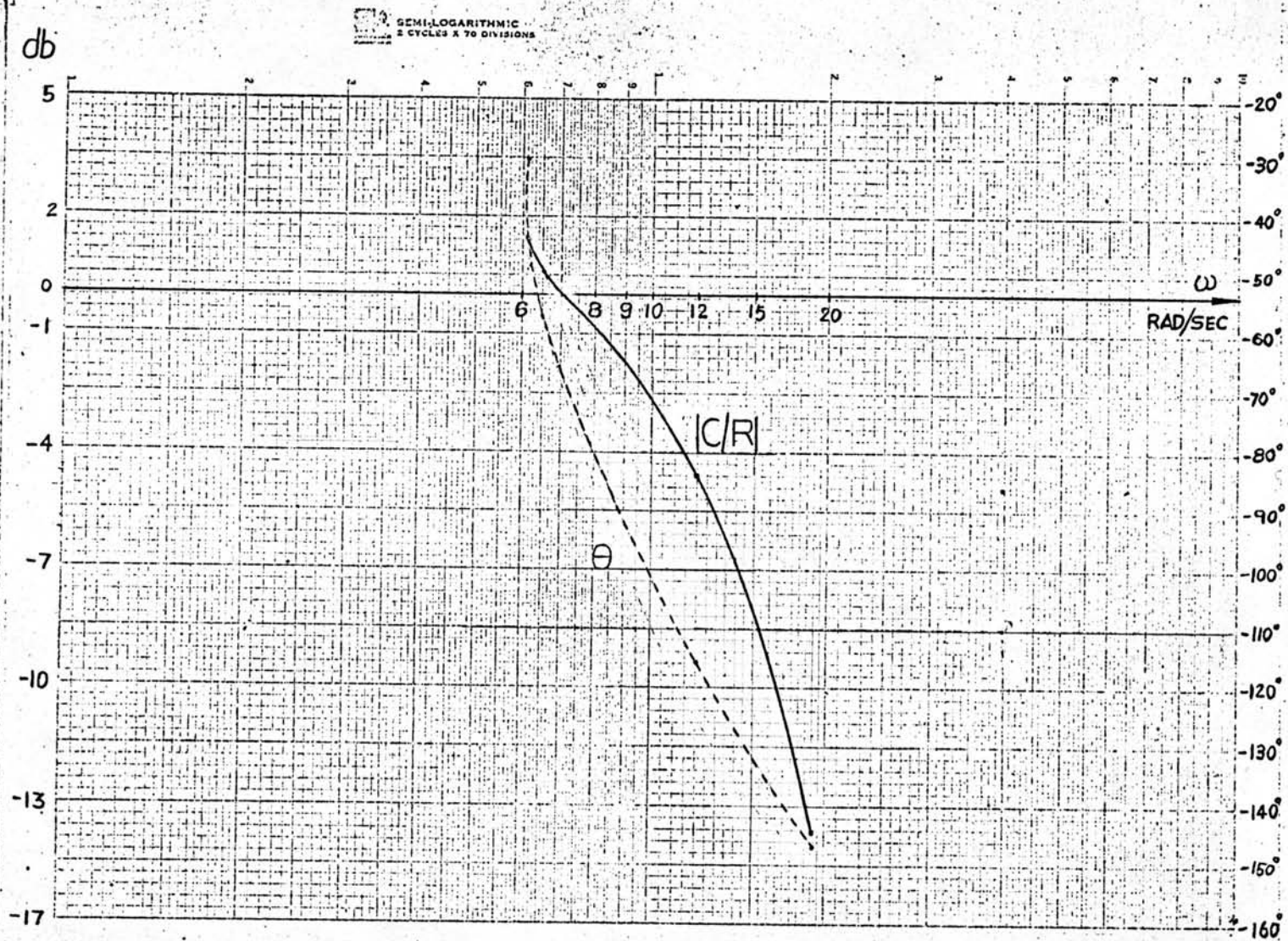


Fig.3.8 Output frequency response of nonlinear system described in Fig.3.5 and 3.6

3.4 Relay with Dead Zone

In a relay control system, the input-output characteristic of a semi-ideal relay known as relay with dead zone or on-off system has appearance of the curve in Fig. 3.9.

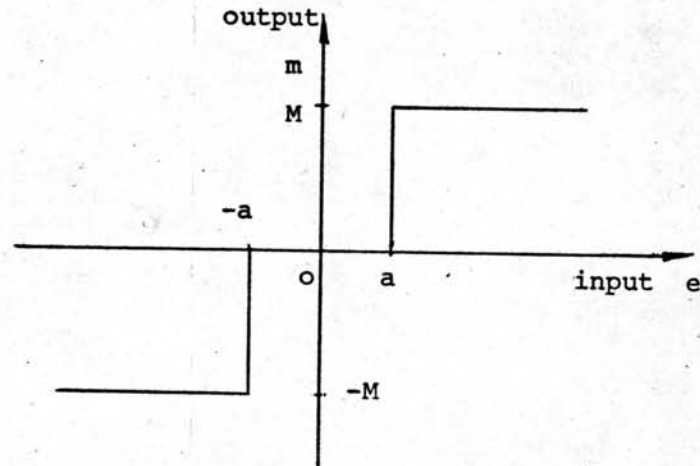


Fig. 3.9 A relay with dead zone characteristic.

3.4.1 Example

Consider a typical nonlinear system as shown in Fig. 3.10.

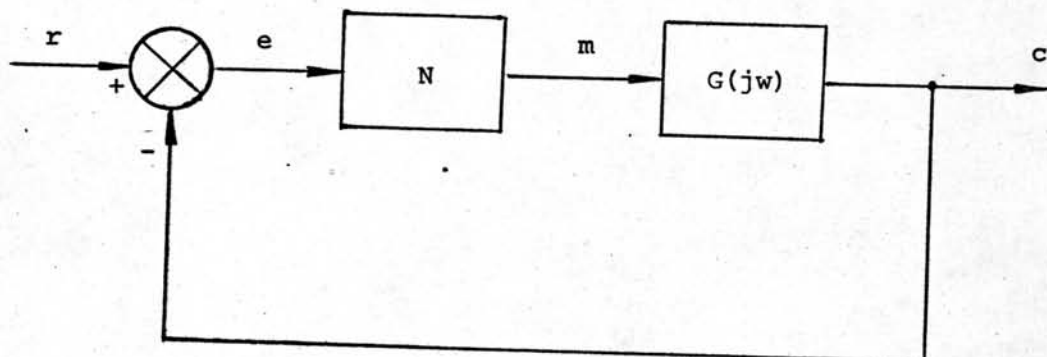


Fig. 3.10 A typical nonlinear system with dead zone.

The input signal, is

$$r = 3.75 \sin \omega t \quad (3.7)$$

The parameters of the characteristic shown in Fig. 3.9 are

$$a = 1.25 \quad (3.8)$$

$$M = 2.50$$

The linear transfer function is

$$G(j\omega) = \frac{20}{j\omega (2j\omega + 1)} \quad (3.9)$$

In this example the family of circle curves and the new linear transfer function, $\frac{G(j\omega)}{a/M}$, are plotted in the same complex graph in Fig. 3.11. The output frequency response of this nonlinear system for various values of frequency ω has been calculated by eqn. (2.13) and also listed in Table 3.3, the output response is also plotted in Fig. 3.12. It can be seen that there is a jump phenomena occurs in this nonlinear system.

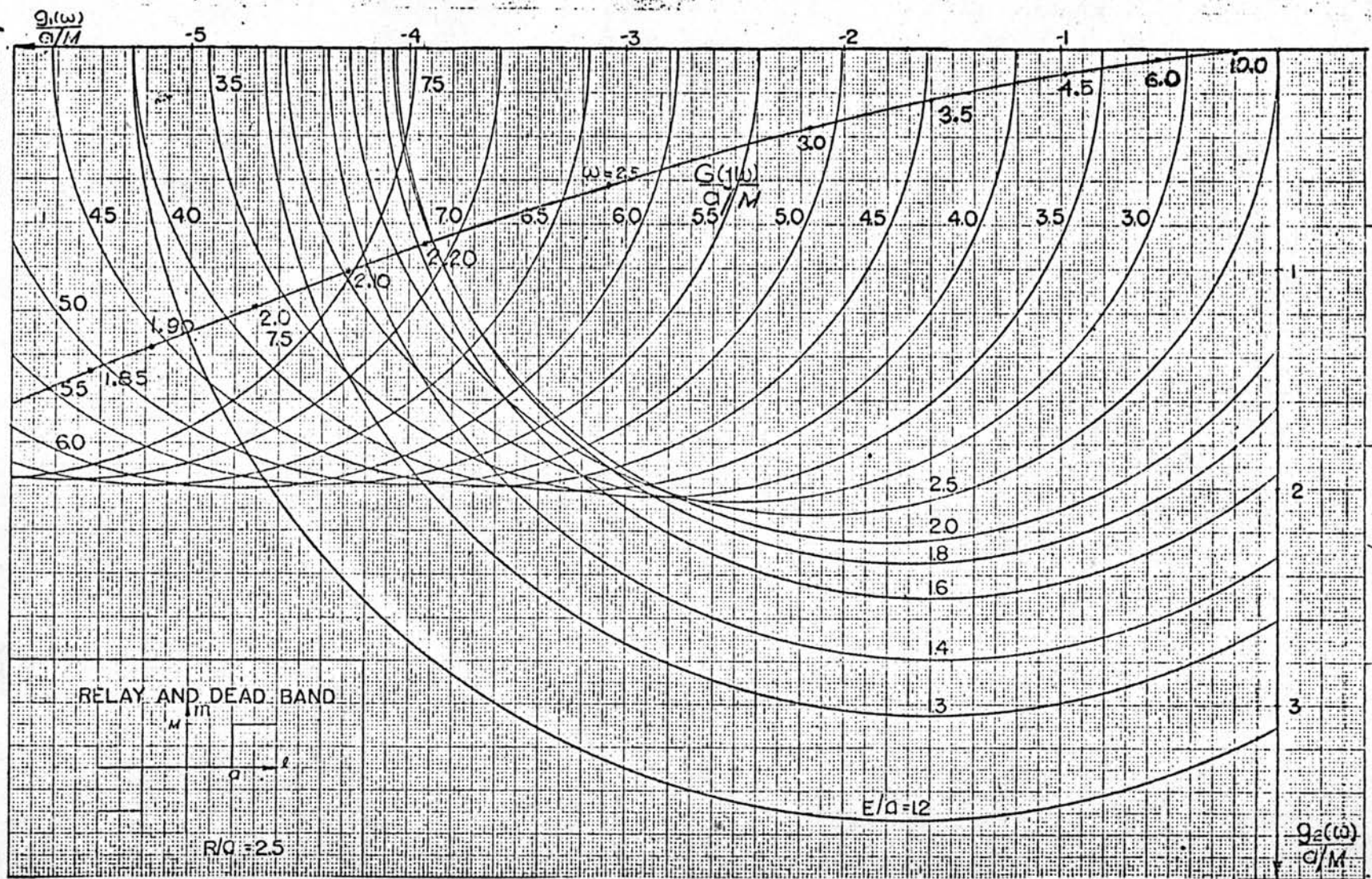


Fig. 3.11 Family of circle curves for relay with dead zone and
 the curve of $G(j\omega) = \frac{20}{j\omega(1+2j\omega)}$

Table 3.3 Calculated results of Example in section 3.4.1

E/a	w	$G(jw)K_{eq}(E)$	$1+G(jw)K_{eq}(E)$	$ C/R $	$ C/R $ db	θ
5.0	1.86	1.39 $\underline{195.0^\circ}$	0.50 $\underline{226.6^\circ}$	2.78	8.88	-31.6°
4.5	1.91	1.46 $\underline{194.7^\circ}$	0.55 $\underline{222.1^\circ}$	2.65	8.46	-27.4°
1.2	1.93	3.04 $\underline{193.9^\circ}$	2.08 $\underline{218.0^\circ}$	1.46	3.29	-24.1°
3.5	2.03	1.65 $\underline{193.7^\circ}$	0.72 $\underline{213.0^\circ}$	2.29	7.20	-19.3°
3.0	2.10	1.77 $\underline{193.4^\circ}$	0.83 $\underline{209.7^\circ}$	2.13	6.57	-16.3°
2.0	2.20	2.20 $\underline{192.9^\circ}$	1.24 $\underline{203.3^\circ}$	1.77	4.96	-10.4
1.8	2.20	2.20 $\underline{192.9^\circ}$	1.24 $\underline{203.3^\circ}$	1.77	4.96	-10.4°
7.0	2.25	0.69 $\underline{192.4^\circ}$	0.35 $\underline{-25.1^\circ}$	1.97	5.89	-142.5°
6.0	2.60	0.60 $\underline{191.5^\circ}$	0.43 $\underline{-16.3^\circ}$	1.40	2.92	-152.2°
5.0	3.10	0.52 $\underline{188.9^\circ}$	0.50 $\underline{-9.3^\circ}$	1.04	0.34	-161.8°
4.0	4.10	0.38 $\underline{187.5^\circ}$	0.62 $\underline{-4.6^\circ}$	0.61	-4.29	-167.9°
3.5	5.10	0.29 $\underline{185.9^\circ}$	0.71 $\underline{-2.4^\circ}$	0.41	-7.74	-171.7°
3.0	7.00	0.17 $\underline{183.4^\circ}$	0.83 $\underline{-0.7^\circ}$	0.20	-13.98	-175.9°

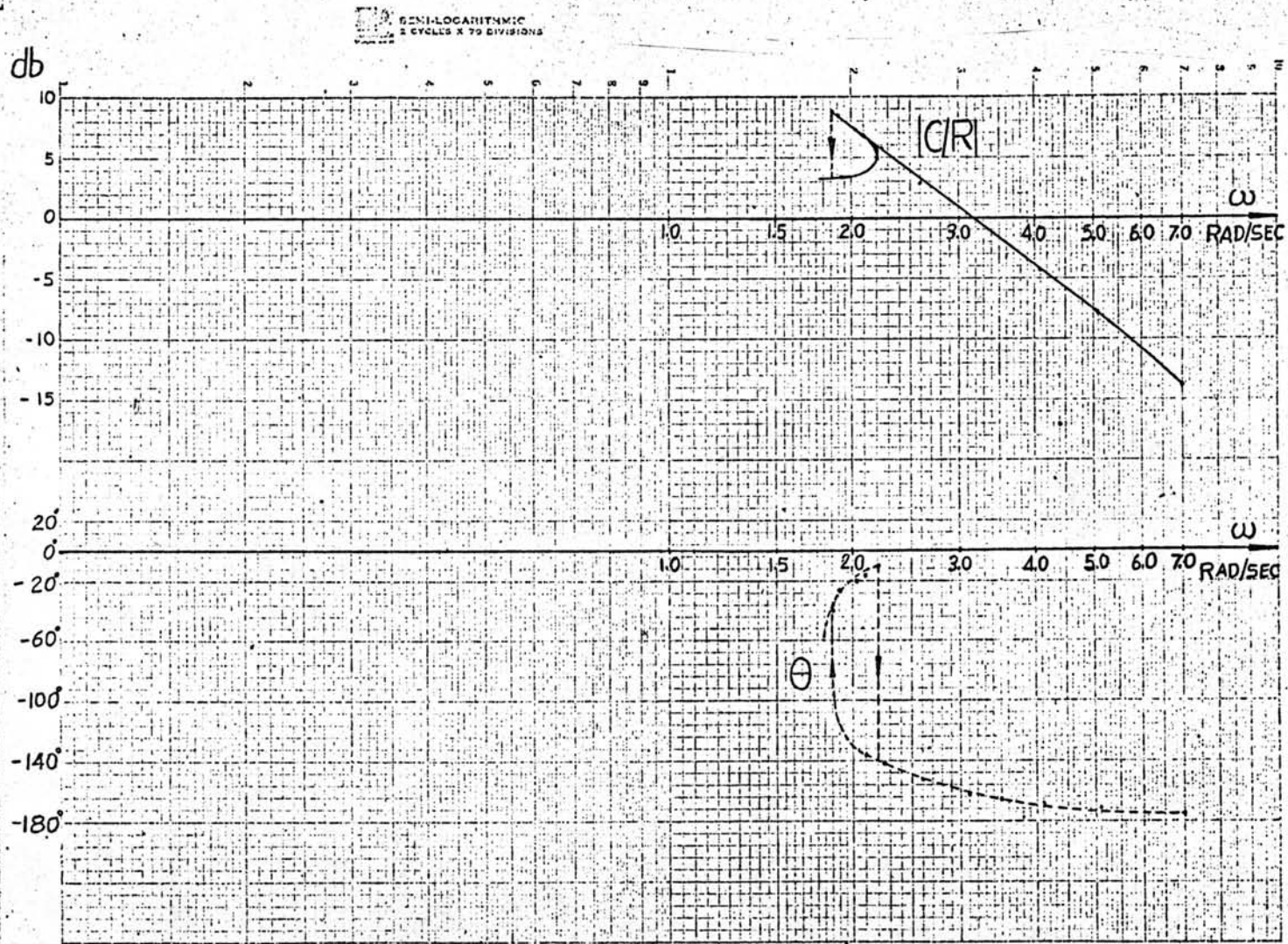


Fig.3.12 Output frequency response of nonlinear system described in Fig.3.9 and 3.10

3.5 Backlash

This type of nonlinearity can be found in gear train used in control systems such as the transmission unit from the servomotor to pressure control unit, pumping system. A backlash characteristic is described in Fig. 3.13.

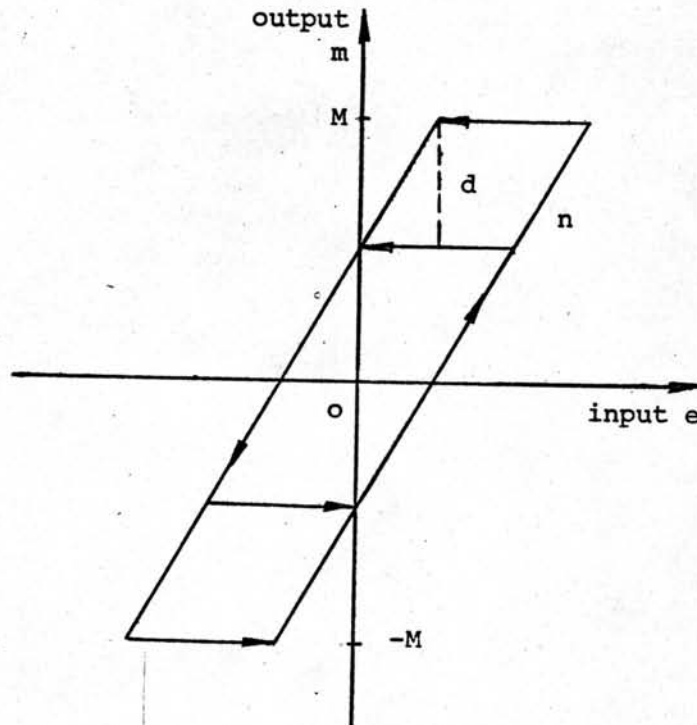


Fig. 3.13 A backlash.

3.5.1 Example

Consider a typical nonlinear system as shown in Fig. 3.14.

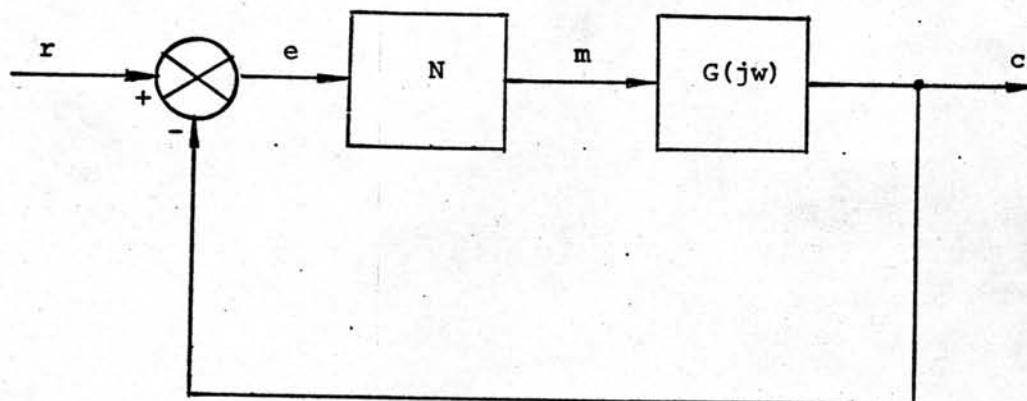


Fig. 3.14 A typical nonlinear system with backlash.

The input signal, is

$$r = 1.5 \sin \omega t \quad (3.10)$$

The parameters of the characteristic shown in Fig. 3.13 are

$$d = 1.0 \quad \text{and} \quad n = 1.0 \quad (3.11)$$

The linear transfer function is

$$G(j\omega) = \frac{500}{j\omega (20 + j\omega)} \quad (3.12)$$

In this example the family of circle curves and the new linear transfer function, $\frac{G(j\omega)}{1/n}$, are plotted in the same complex graph in Fig. 3.15. The output frequency of this nonlinear system for various values of frequency ω has been calculated by eqn. (2.13) and also listed in Table 3.4. The output response is also plotted in Fig. 3.16. It can be seen that there is no jump response phenomena occurs in this type of nonlinear system.

I1b01bAAA

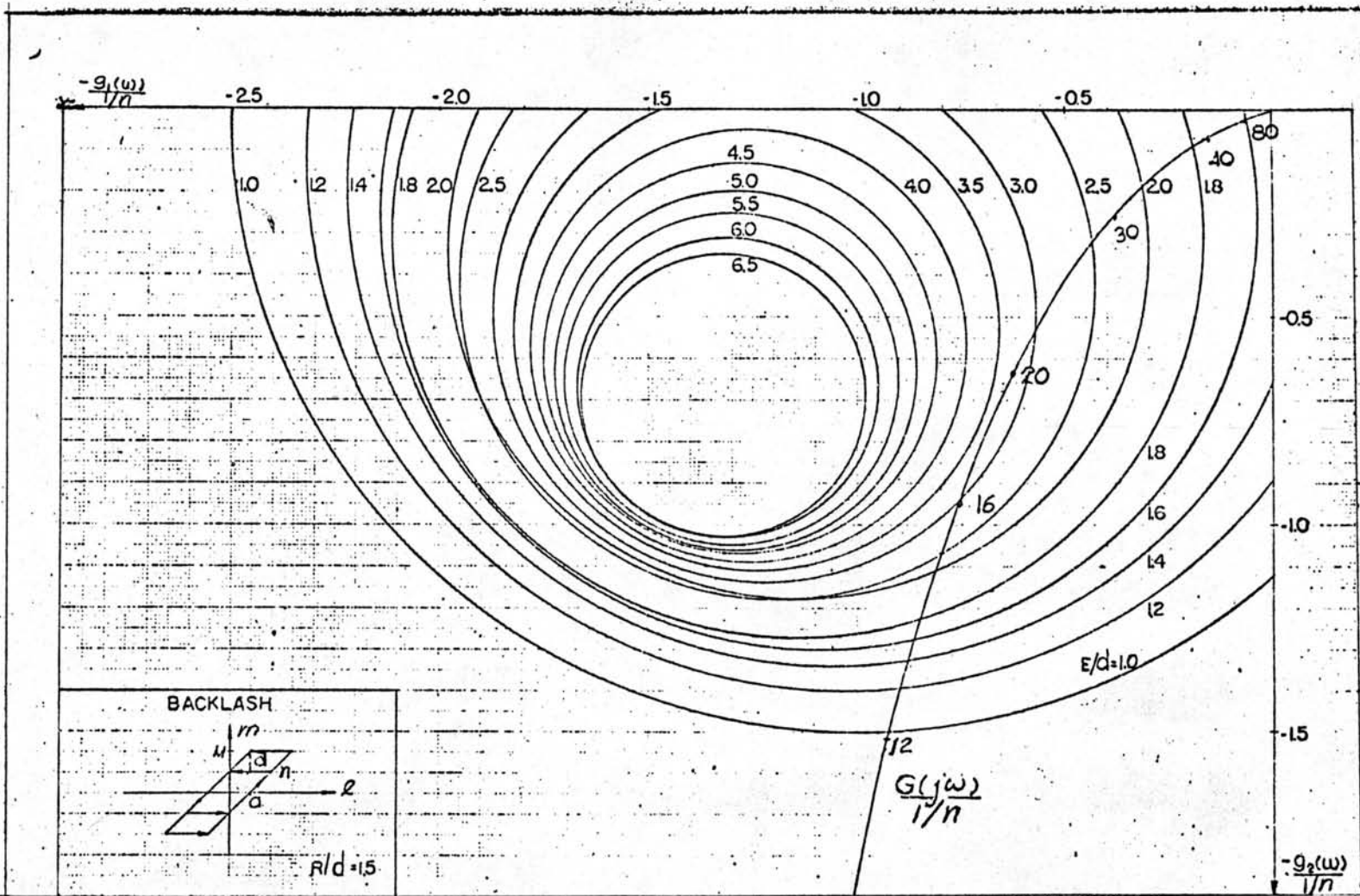


Fig. 3.15 Family of circle curves for backlash and the curve of $G(j\omega) = \frac{500}{j\omega(20+j\omega)}$

Table 3.4 Calculated results of example in section 3.5.1

E/d	w	$G(j\omega)K_{eq}(E)$	$1+G(j\omega)K_{eq}(E)$	$ C/R $	$ C/R $ db	θ
1.0	12.2	1.76 \angle -136.4°	1.50 \angle -88.3°	1.17	1.36	-48.1°
1.6	13.5	1.37 \angle -137.4°	0.93 \angle -89.4°	2.73	8.72	-48.0°
3.0	16.2	0.93 \angle -150.9°	0.49 \angle -67.1°	1.90	5.58	-83.8°
3.0	22.1	0.59 \angle -159.1°	0.50 \angle -25.0°	1.18	1.44	-134.1°
2.0	33.5	0.31 \angle -165.1°	0.70 \angle -6.5°	0.44	-7.13	-158.6°
1.6	80.0	0.06 \angle -170.5°	0.94 \angle -0.6°	0.06	-24.44	-169.9°

SEMI-LOGARITHMIC
2 CYCLES X 70 DIVISIONS

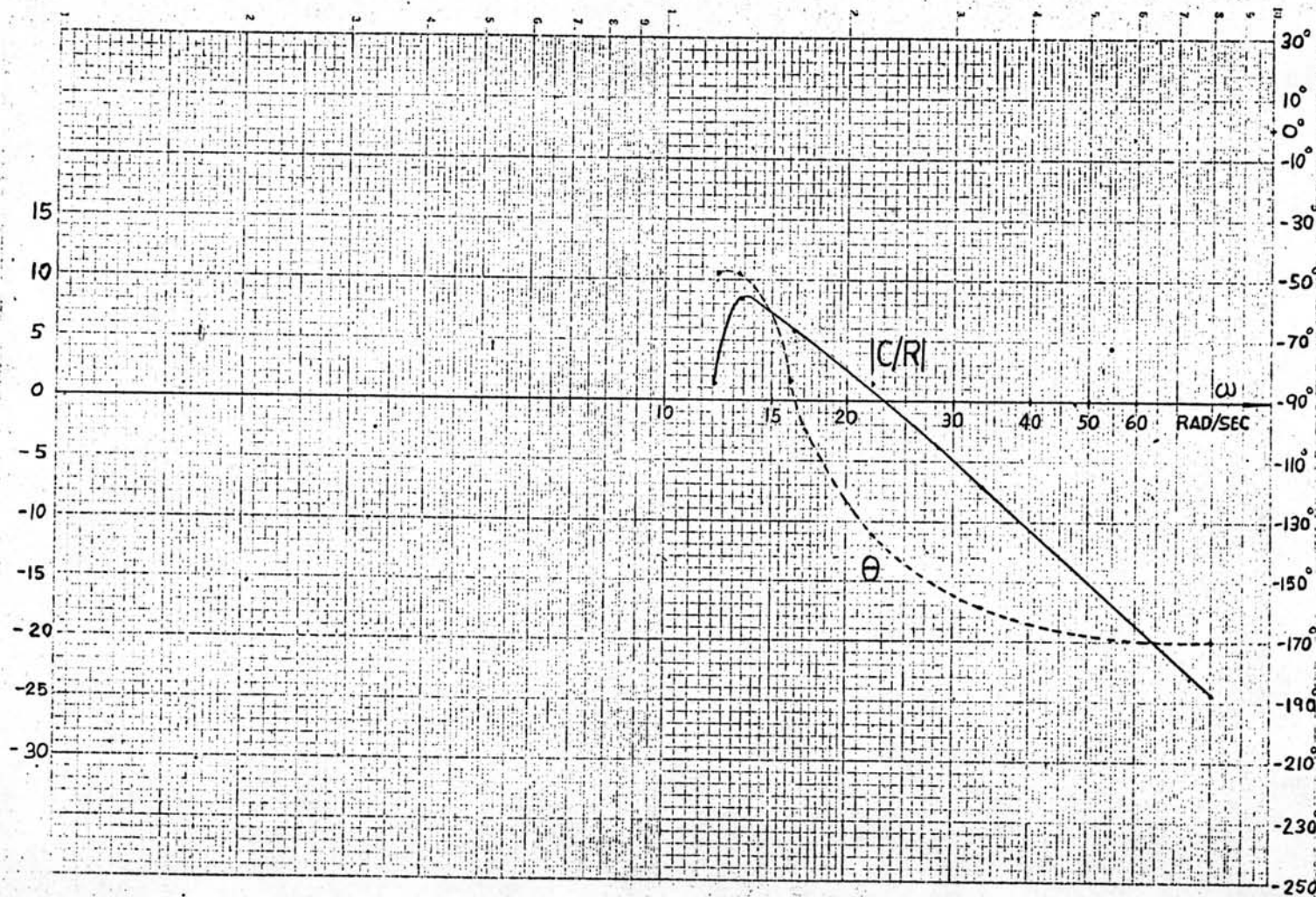


Fig.3.16 Output frequency response of nonlinear system described in Fig.3.13 and 3.14

3.6 Saturation

No physical component can generate a continually increasing quantity. The device reaches a physical limit, such as a mechanical stop of fuse, beyond which it will not operate. Fig. 3.17 shows how even a linear relationship can reach this cut off condition, known as saturation.

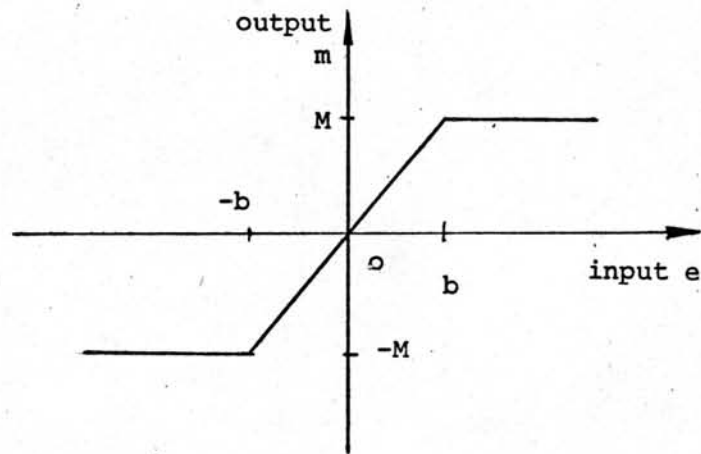


Fig. 3.17 Saturation.

3.6.1 Example

Consider a typical nonlinearity system as shown in Fig. 3.15.

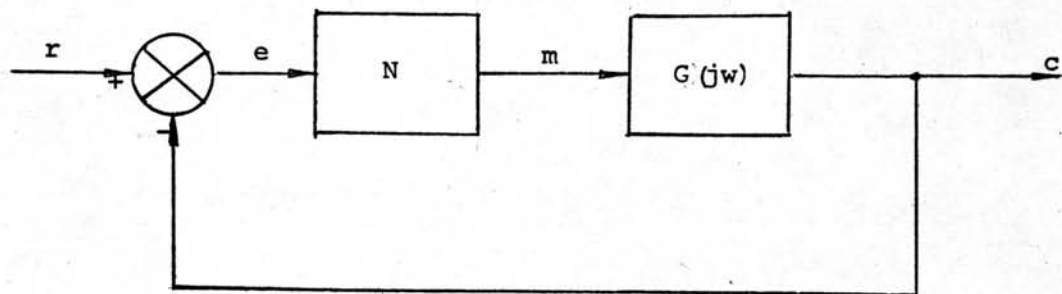


Fig. 3.18 A typical nonlinear system with saturation.

The input signal, is

$$r = 1.5 \sin \omega t \quad (3.13)$$

The parameters of the nonlinear characteristic are

$$\left. \begin{aligned} n &= 1.0 \\ b &= 1.0 \\ M &= 1.0 \end{aligned} \right\} \quad (3.14)$$

The linear transfer function is

$$G(j\omega) = \frac{100}{j\omega (10 + j\omega)} \quad (3.15)$$

In this example the family of circle curves and the new linear transfer function, $\frac{G(j\omega)}{1/n}$, are plotted in the same complex graph in Fig. 3.19. The output frequency response of this nonlinear system for various values of frequency ω has been calculated by eqn. (2.13) and also listed in Table 3.5. The output frequency response is also plotted in Fig. 3.20. It can be seen that the jump response phenomena is not occurred in this example.

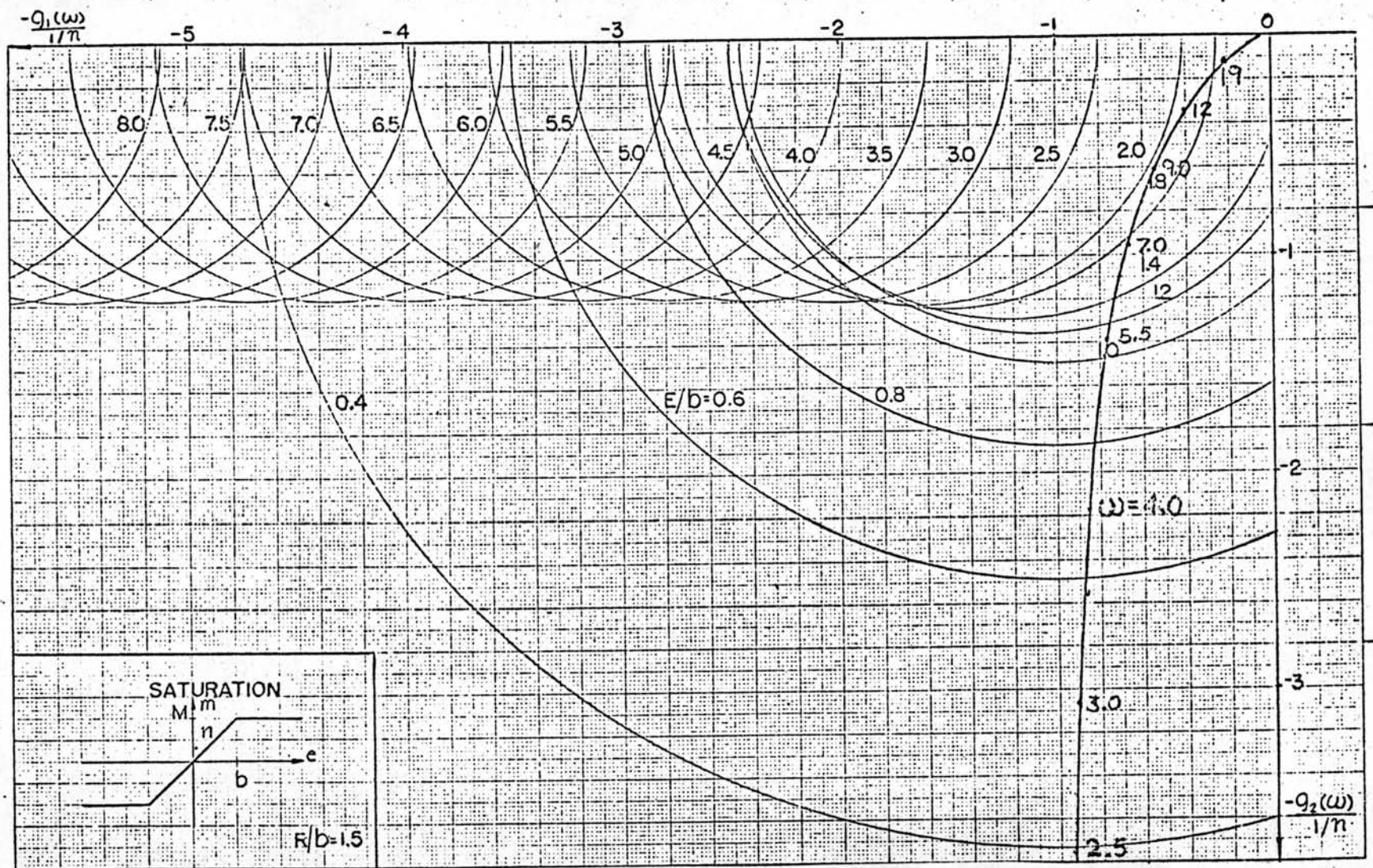


Fig. 3.19 Family of circle curves for saturation and the curve of $G(j\omega) = \frac{100}{j\omega(10+j\omega)}$

Table 3.5 Calculated results of example in section 3.6.1.

E	w	$G(j\omega)K_{eq}(E)$	$1+G(j\omega)K_{eq}(E)$	$ C/R $	$ C/R $ db	θ°
0.4	2.51	3.85 $\angle 256.0^\circ$	3.74 $\angle -88.9^\circ$	1.03	0.26	-15.1°
0.6	3.56	2.63 $\angle 250.5^\circ$	2.48 $\angle -87.2^\circ$	1.06	0.51	-22.3°
0.8	4.45	2.04 $\angle 246.0^\circ$	1.87 $\angle -84.8^\circ$	1.09	0.75	-29.2°
1.2	5.7	1.40 $\angle 240.0^\circ$	1.25 $\angle -76.1^\circ$	1.12	0.98	-43.9°
1.8	7.2	0.76 $\angle 234.6^\circ$	0.84 $\angle -47.9^\circ$	0.90	-0.92	-77.5°
1.8	18.0	0.21 $\angle 215.2^\circ$	0.84 $\angle -8.2^\circ$	0.25	-12.0	-136.6°

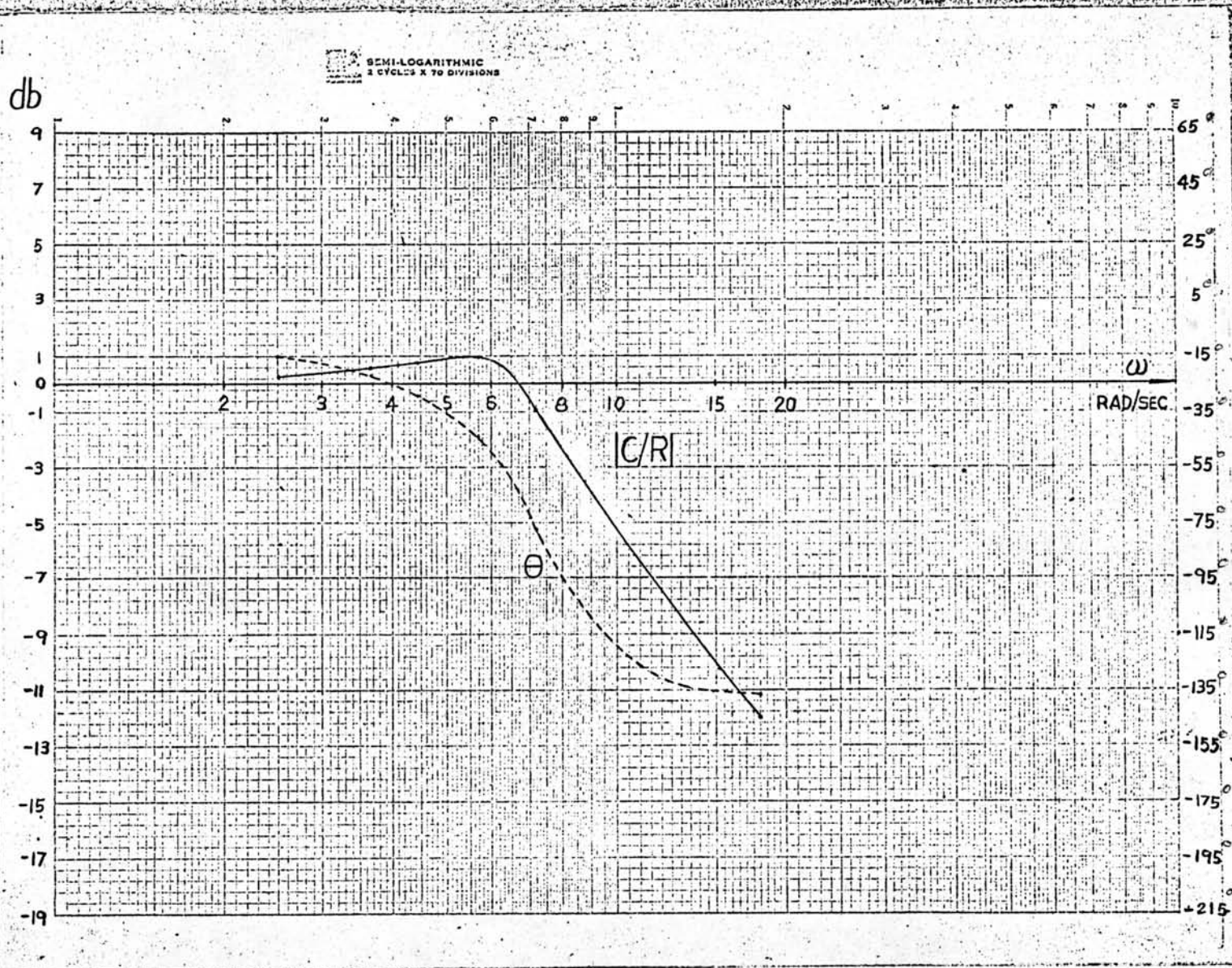


Fig. 3.20 Output frequency response of nonlinear system described in Fig. 3.17 and 3.18

3.7 Simulations

The analogue computer simulations of typical nonlinear systems as mentioned in the section 3.3 and 3.6 have been carried out on the Yew analogue computer in order to verify the analytical solutions as presented in the previous sections.

3.7.1 Analogue computer simulation I

The nonlinear system which consists of an ideal relay characteristic linear transfer function, and the input signal as described in section 3.3 has been simulated by using the Yew analogue computer. The analogue computer set up has shown in the Fig. 3.21.

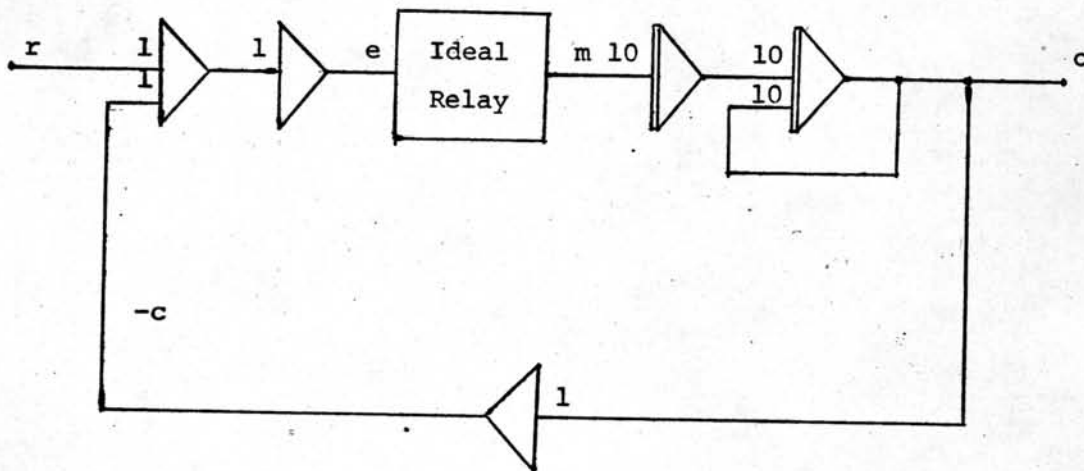


Fig. 3.21 An analogue computer diagram for the nonlinear system described in section 3.3.

In this case the ideal relay can be simulated as shown in Fig. 3.22.

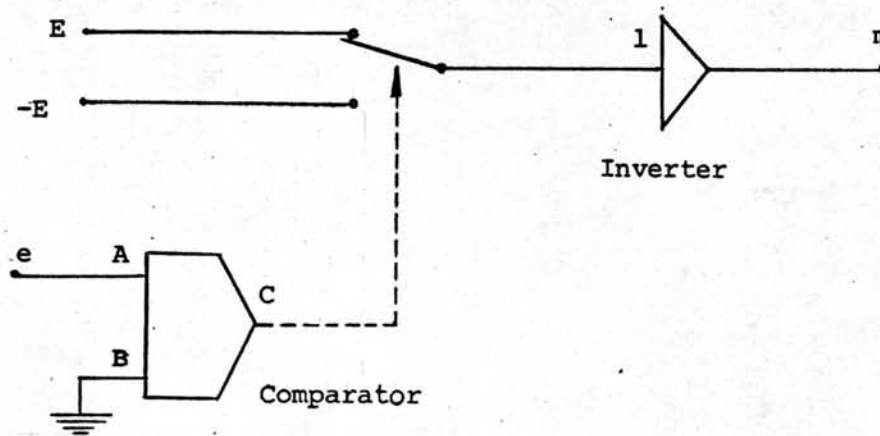


Fig. 3.22 An analogue computer diagram for an ideal relay simulation.

when the input is an sinusoidal signal, we have

$$r = 1.5 \sin \omega t \quad (3.16)$$

The nonlinear characteristic output m may be expressed as

$$\left. \begin{aligned} m &= E = 1.0 \text{ v} && \text{for } e > 0 \\ m &= -E = -1.0 \text{ v} && \text{for } e < 0 \end{aligned} \right\} (3.17)$$

The input signal and typical waveforms of the output frequency responses of the nonlinear system shown in Fig. 3.21 have been given in Fig. 3.23 (a), (b) and (c) respectively.

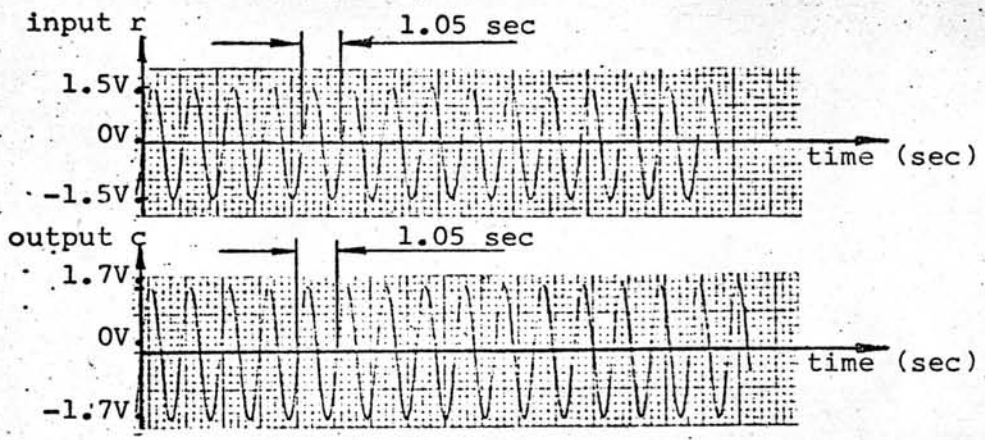


Fig.3.23a Input and output waveforms at frequency 0.95 cps

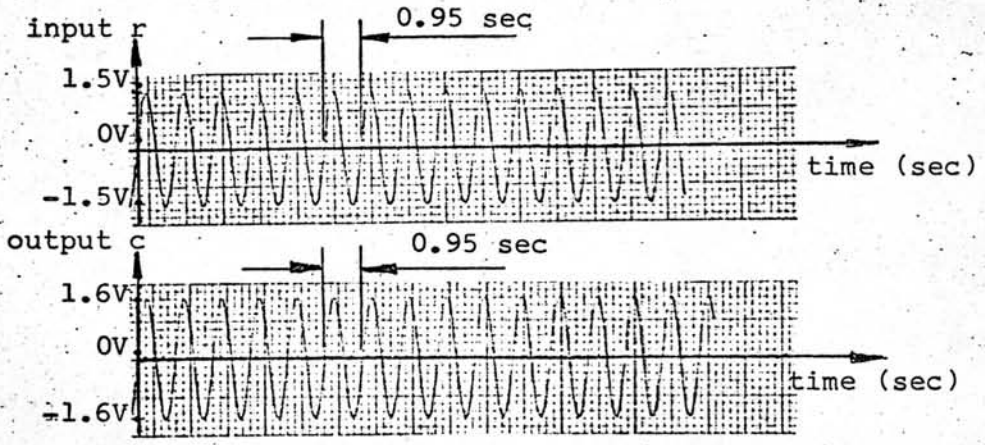


Fig.3.23b Input and output waveforms at frequency 1.05 cps

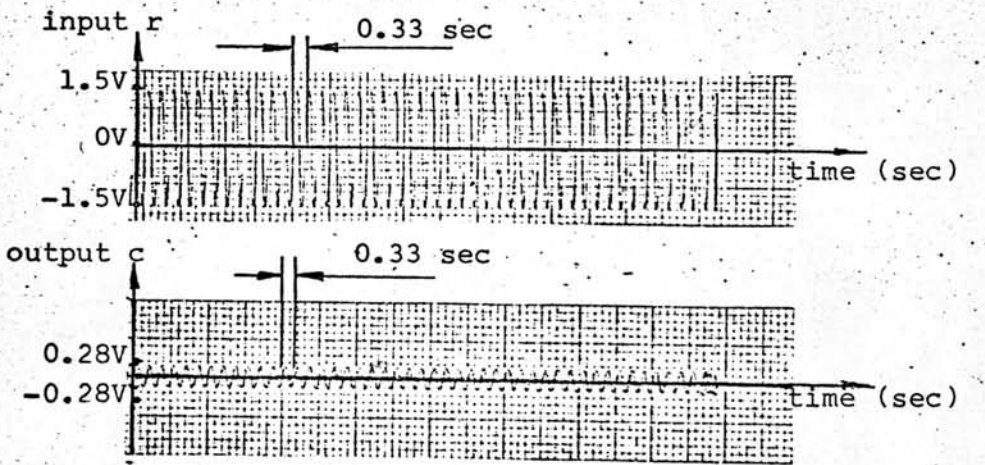


Fig.3.23c Input and output waveforms at frequency 3.00 cps

Fig.3.23 Input and typical output waveforms at various frequencies.

The output frequency responses from the calculated results obtained from section 3.3 and simulated results are plotted in Fig. 3.24. It can be seen from this figure that both simulated and calculated results are close together. This give a sound confidence to use the graphical method to calculate the approximate output frequency response.

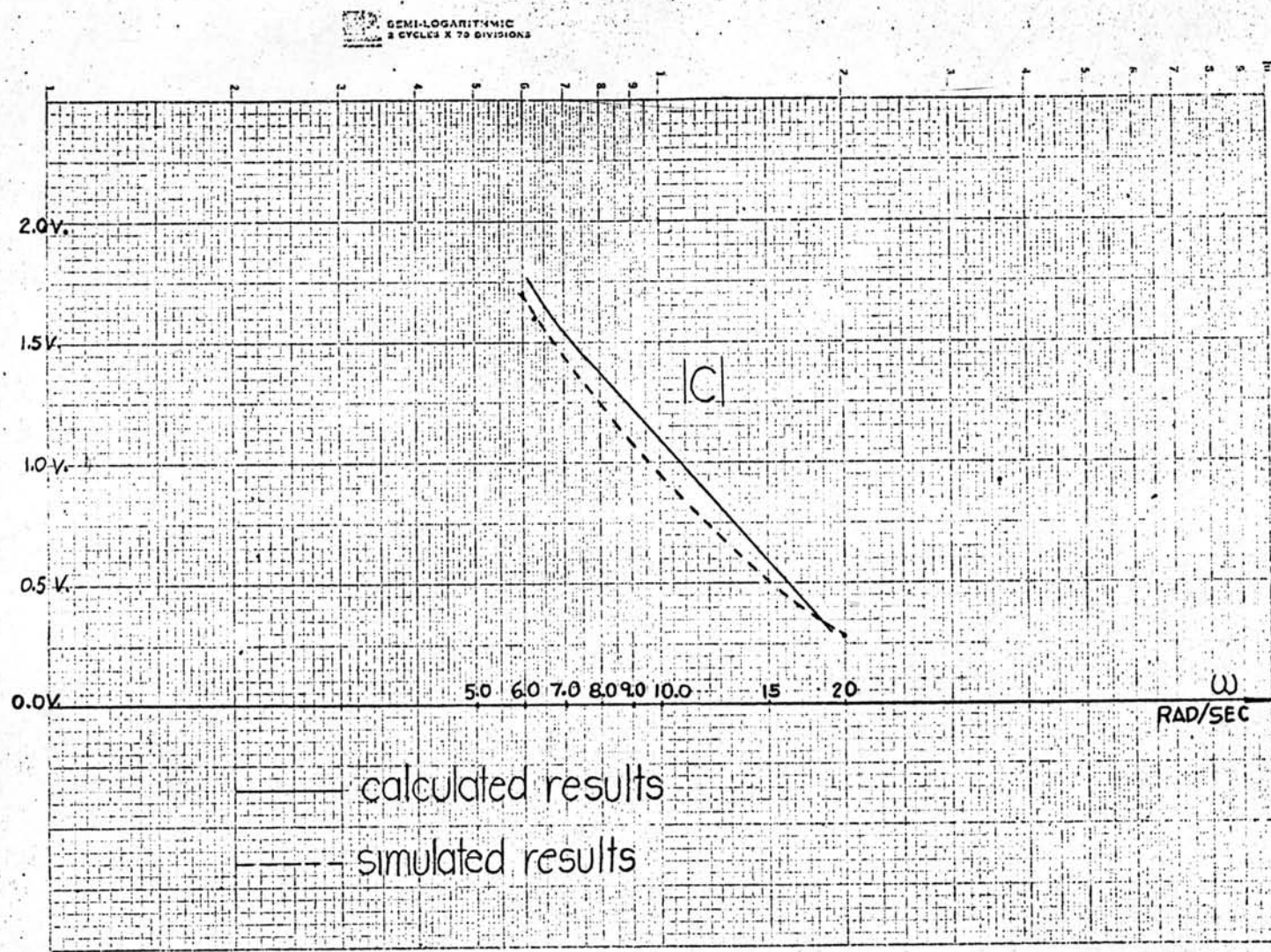


Fig.3.24 Output frequency responses for the calculated results from section 3.3 and simulated results from section 3.7.1

3.7.2 Analogue computer simulation II

The nonlinear system which consist of a saturation characteristic, linear transfer function and the input signal as described in section 3.6 has been simulated by the Yew' analogue computer as shown in Fig. 3.25.

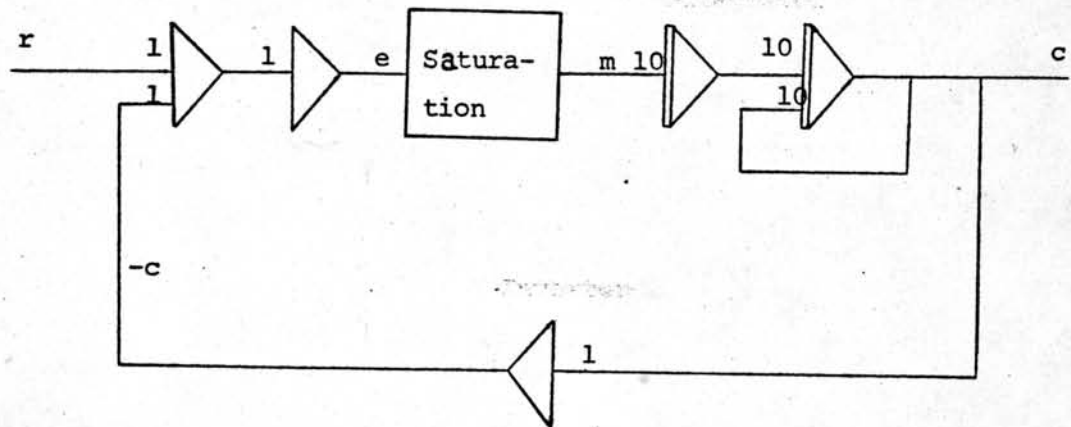


Fig. 3.25 An analogue computer diagram for the nonlinear system described in section 3.6.

In this case the saturation can be simulated as shown in Fig. 3.26.

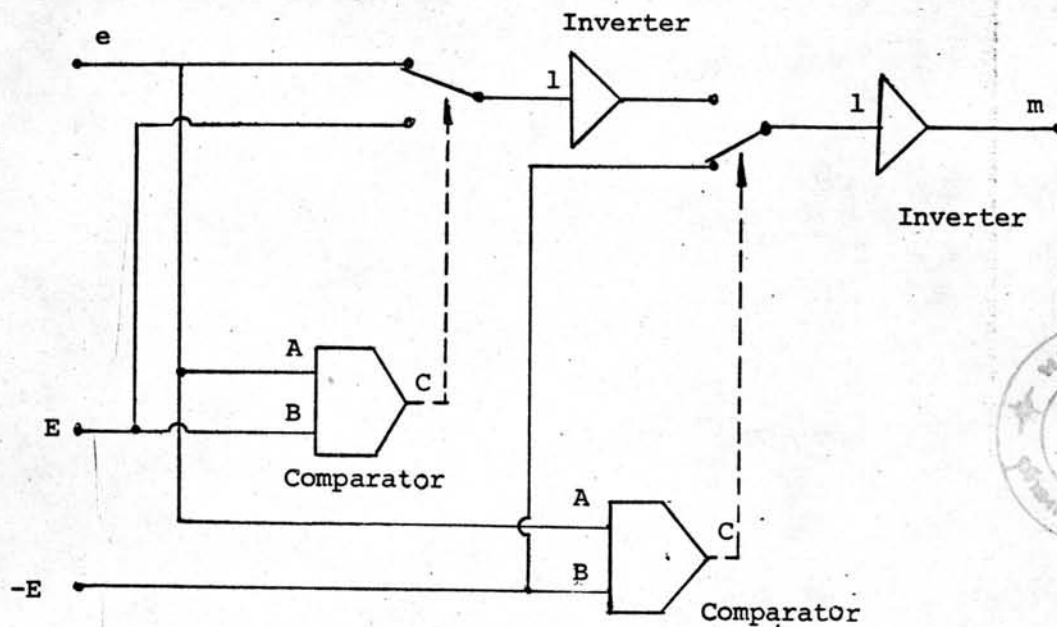


Fig. 3.26 An analogue computer diagram for a saturation simulation.

When the input is a sinusoidal signal, we have

$$r = 1.5 \sin \omega t \quad (3.18)$$

In this case output m may be expressed as

$$\left. \begin{aligned} m &= E = 1.0 \text{ V.} && \text{for } e > 1 \\ m &= e \text{ V.} && \text{for } -1 \leq e \leq 1 \\ m &= -E = -1.0 \text{ V.} && \text{for } e < -1 \end{aligned} \right\} (3.19)$$

The input signals and typical waveforms of the output frequency responses have been given in Fig. 3.27 (a), (b), (c), (d), (e) and (f) respectively.

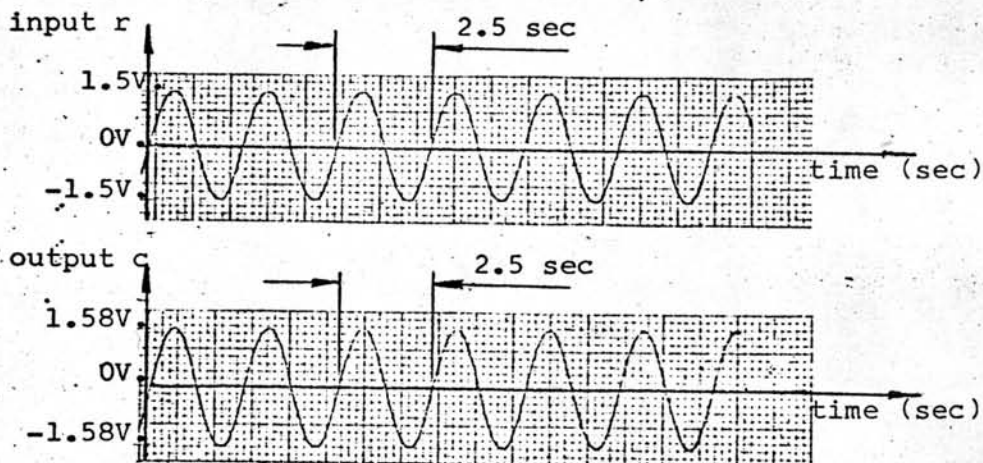


Fig.3.27a Input and output waveforms at frequency 0.40 cps

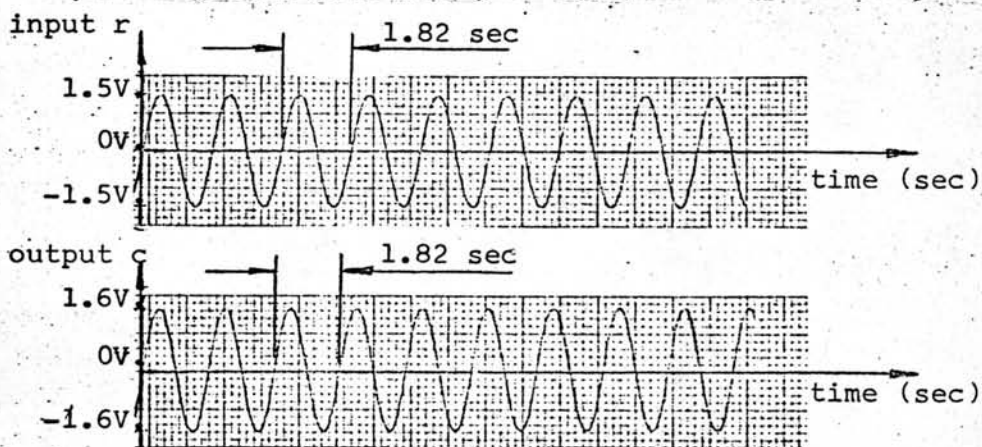


Fig.3.27b Input and output waveforms at frequency 0.55 cps

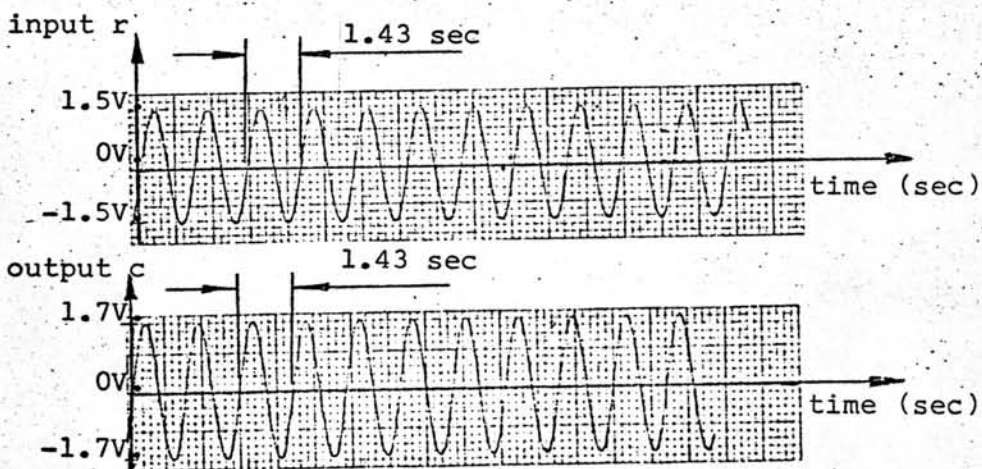


Fig.3.27c Input and output waveforms at frequency 0.70 cps

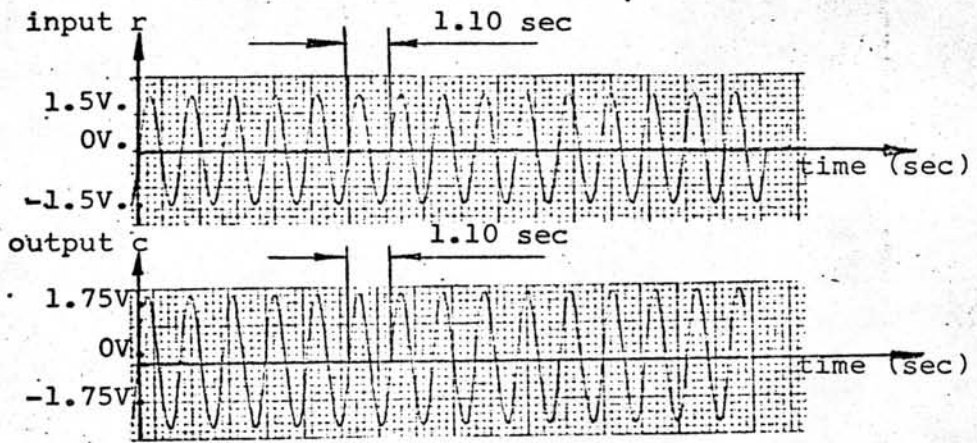


Fig.3.27d Input and output waveforms at frequency 0.90 cps

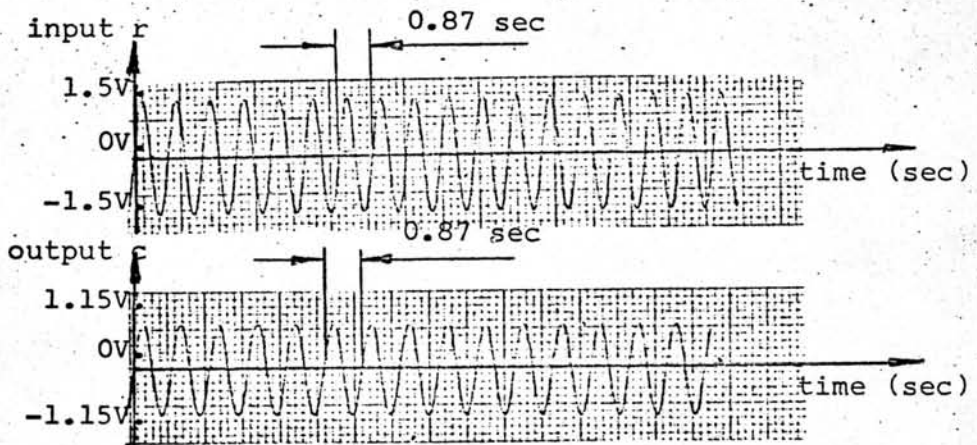


Fig.3.27e Input and output waveforms at frequency 1.15 cps

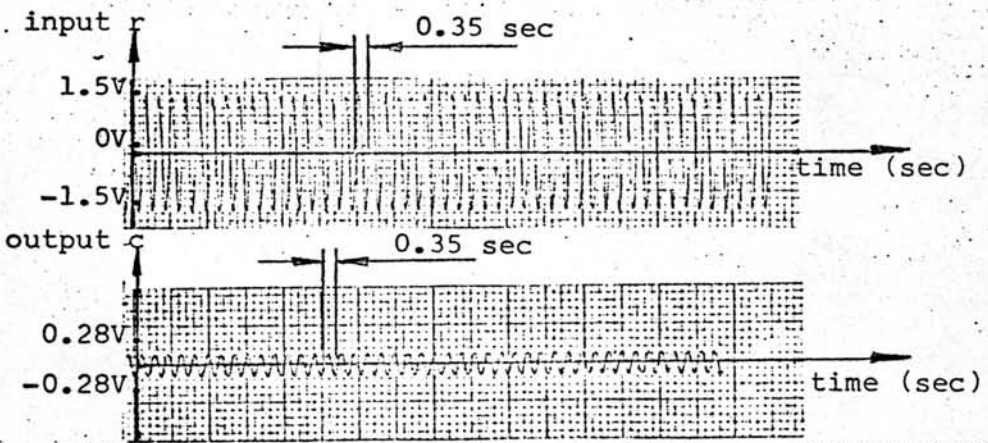


Fig.3.27f Input and output waveforms at frequency 2.85 cps

Fig.3.27 Input and typical output waveforms at various frequencies

The output frequency response of the simulated results and calculated results obtained from section 3.6 have been plotted in Fig. 3.28.

It can be seen from this figure that both simulated and calculated results for the output frequency response of this non-linear system are also close together. Therefore we may conclude that the graphical method presented in this thesis is a practical method for determination of the frequency response of the typical nonlinear system.

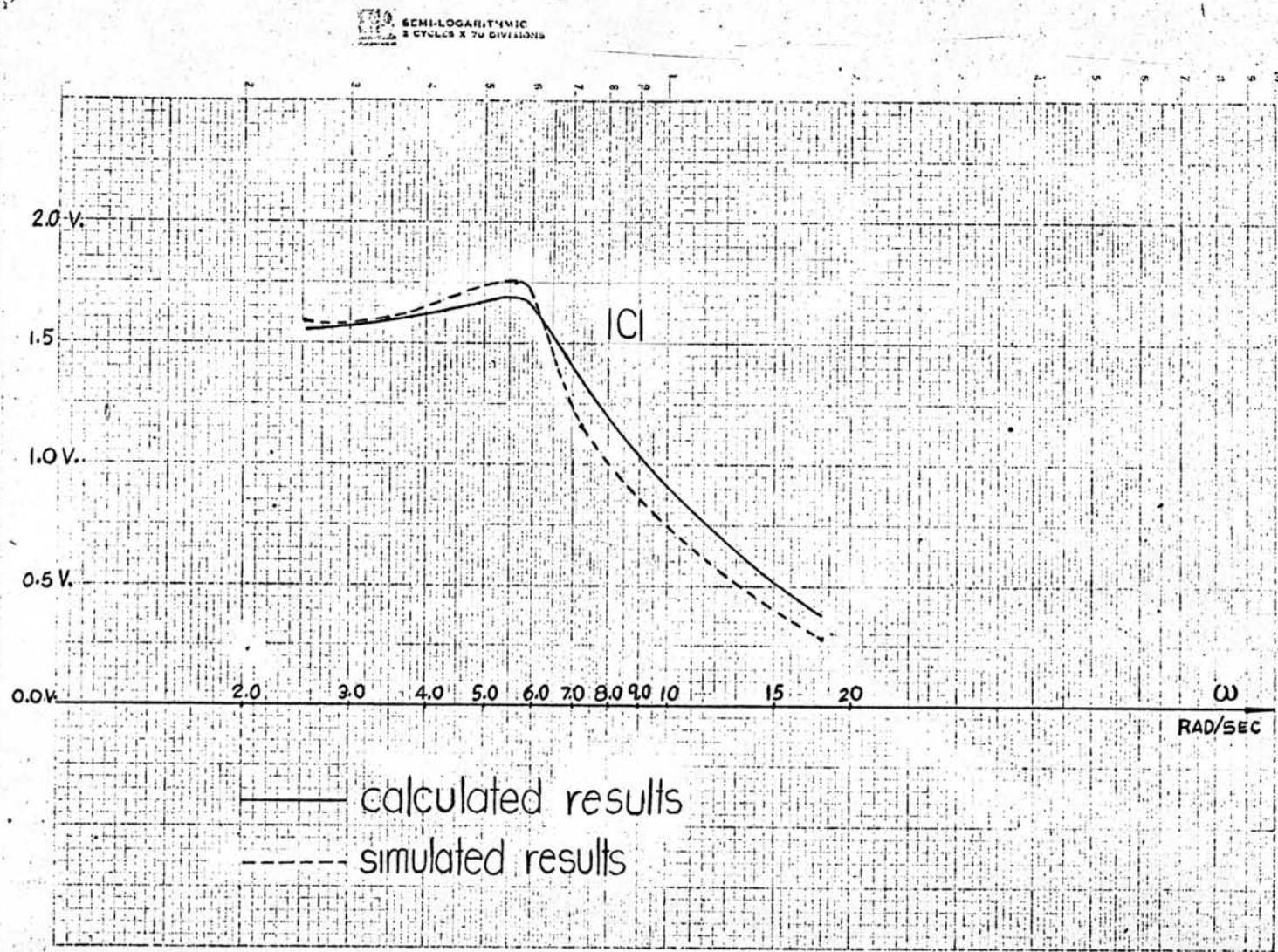


Fig.3.28 Output frequency responses for calculated results from section 3.6 and simulated results from section 3.7.2